NASA Technical Memorandum 79168

ASSESSMENT AT FULL SCALE OF NOZZLE/WING GEOMETRY EFFECTS ON OTW AERO-ACOUSTIC CHARACTERISTICS

D. Groesbeck and U. von Glahn
Lewis Research Center
Cleveland, Ohio

Prepared for the
Ninety-seventh Meeting of the Acoustical Society of America
Cambridge, Massachusetts, June 11-15, 1979

ASSESSMENT AT FULL SCALE OF NOZZLE/WING GEOMETRY EFFECTS ON OTW AEROACOUSTIC CHARACTERISTICS

by D. Groesbeck and U. von Glahn

National Aeronautics and Space Administration
Lewis Research Center
Cleveland, Ohio

ABSTRACT

The effects on acoustic characteristics of nozzle type and location on a wing for STOL engine over-the-wing configurations are assessed at full scale on the basis of model-scale data. Three types of nozzle configurations are evaluated: a circular nozzle with external deflector mounted above the wing, a slot nozzle with external deflector mounted on the wing and a slot nozzle mounted on the wing. Nozzle exhaust plane locations with respect to the wing leading edge are varied from 10 to 46 percent chord (flaps retracted) with flap angles of 20° (take-off attitude) and 60° (approach attitude). Perceived noise levels (PNL) are calculated as a function of flyover distance at 152 m altitude. From these plots, static EPNL values, defined as flyover relative noise levels, are calculated and plotted as a function of lift and thrust ratios. From such plots the acoustic benefits attributable to variations in nozzle/deflector/wing geometry at full scale are assessed for equal aerodynamic performance.

INTRODUCTION

One concept advanced for STOL aircraft features mounting the engines over the wing (OTW). Such an installation directs the jet exhaust over the upper surface of the wing/flap system, thereby augmenting the wing lift by providing an additional lift component. Furthermore, the wing/flap system provides shielding of some high frequency jet exhaust noise although generating additional low frequency jet/surface interaction noise. The latter does not contribute significantly to the community noise problem, although it can cause local structural problems and increase cabin interior noise.

The attachment of the jet exhaust to the wing/flap for lift augmentation can be achieved in several ways. One of the more commonly considered concepts is the use of a slot or a D-shaped nozzle mounted directly on the upper surface of the wing (fig. 1(a)). Another concept consists of a nozzle with an external flow deflector. This deflector vectors the exhaust flow toward the wing for attachment

to the wing/flap surfaces. During cruise, the deflector is stored in the engine nacelle or in the upper surface of the wing. During the landing procedure, such a deflector has the possibility of being used as a thrust reverser. Representative configurations making use of external flow deflectors are shown in figures 1(b) and (c).

Initial work on the engine over-the-wing concept at NASA Lewis Research Center (1971) consisted of 1/13-scale model studies. The associated model-scale nozzles in these and subsequent works, for the most part, had a nominal 5.1 cm equivalent diameter. The model-scale nozzles were tested in conjunction with wings having chords of 22.0, 33.0, and 49.5 cm (flaps retracted). In the present study, the model-scale data are extrapolated to the full-scale nozzle equivalent diameter of 66 cm (13:1 scale), with the corresponding scaling of the wing/flap system for each configuration. Jet exhaust velocities ranged from a nominal 195 m/s to a nominal 260 m/s. The three nozzle concepts illustrated in figure 1 are evaluated at full scale in terms of a flyover relative noise level (defined in appendix A) at a flyover altitude of 152 m. Both approach and takeoff modes are considered. The noise evaluations are made for nozzle/wing configurations having substantially the same lift and thrust. The results obtained in this manner provide an estimation of the aeroacoustic benefits and disadvantages associated with the different nozzle design concepts and operating modes.

APPARATUS AND PROCEDURE

Facilities

Aerodynamic facility. - Aerodynamic data consisting of lift and thrust components were obtained using the test stand described in reference 1. In this test stand, pressurized air at about 290 K was supplied to a 15.2-cm diameter pipe (plenum) by twin, diametrically opposed supply lines. Flexible couplings in each of the twin supply lines isolate the supply system from a force measuring system. The plenum was free to move axially and laterally through an overhead cable suspension system. The test nozzles, with and without wings, were attached to a flange at the downstream end of the plenum. A load cell at the upstream end of the plenum was used to measure thrust. A second load cell was mounted near the nozzle to measure horizontal side loads. The wing-flap section was mounted in a vertical plane so that lift forces were measured by the side-mounted load cell.

Thrust and lift forces were obtained at nominal jet exhaust velocities of 195 and 260 m/s. Airflow through the overhead supply line was measured with a calibrated orifice. The nozzle inlet total pressure was set and measured with a single centerline probe near the plenum exit flange. Pressure data were obtained from suitable multitube and U-tube manometers.

Acoustic facility. - The acoustic data were taken at the outdoor facility described in reference 2. In this facility, dry pressurized, ambient temperature air was supplied to the nozzle/wing configurations through a control valve and valve-noise quieting system. This system consisted of a perforated plate, a four-chamber baffled muffler, and approximately 4.6 m of 10.2 cm diameter piping. Nozzle inlet total pressure was measured with a total-pressure probe.

Acoustic data were obtained with a horizontal nominal 3.0-m radius semicircular array of microphones centered on the nozzle exhaust plane. The 1.27-cm omnidirectional condenser microphones used were in a plane level with the nozzle centerline. The microphones were located at 20°, 40°, 60°, 80°, 90°, 100°, 120°, and 140° measured from the inlet axis. A mat of 15 cm thick urethane foam was placed on the ground (asphalt) inside the microphone array to minimize ground reflections. The microphones were a nominal 1.5 m above ground level.

Acoustic measurements were taken for approximately the same jet exhaust velocities as those for the aerodynamic measurements; that is, 195 and 260 m/s (jet Mach numbers of 0.6 and 0.8, respectively). All flow data for the acoustic tests were taken at cold-flow, ambient temperatures near 290 K.

Microphone output signals were analyzed by a 1/3-octave-band spectrum analyzer. The analyzer provided sound pressure level (SPL) spectra referenced to 2×10^{-5} N/m^2. Overall sound power levels (OASPL) referenced to 10^{-13} watts were computed from the SPL data. Three noise data samples were taken at each microphone location for each pressure ratio. An atmospheric attenuation was applied to the average of the three samples to give lossless data at 3 m. No ground reflection corrections were made to the noise data. The model scale data were then scaled to full size by the appropriate factors for size, flyover distance, and atmospheric attenuation. The full-scale flyover distance was 152 m and the full-scale equivalent nozzle diameter was 66 cm (scale factor, 13:1).

Nozzles

Slot. - The basic slot nozzles (ref. 2) used in the program consisted of the 5:1 nozzles shown in figure 2. These nozzles had equivalent diameters of 5.1 cm. A single straight-sided nozzle was used for the tests without nozzle sidewall cutback. The roof angle, β, of this nozzle was varied by providing inserts that altered the internal angle from 10° to 40° in 10° increments. Separate nozzles were provided for the cases with sidewall cutback. The sidewall cutback angle, γ, was the same as the roof angle for each respective nozzle.

Slot/deflector. - A 5:1 slot nozzle (fig. 3) was used with various external plate-type deflectors that turned the flow in order to provide flow attachment to

the flap. Each of the nozzle sides converged at a 5° angle. The nominal dimensions of the nozzle at the exhaust plane were 2.0 by 10.2 cm. The dimensions of the various deflectors are summarized in the table given in figure 3.

Circular/deflector. - The conical nozzle (fig. 4) used in the study had a 5.2 cm exhaust diameter. Each flow deflector was held in place by two frames or "tracks" fastened to the nozzle. The deflector could be pivoted to various angles relative to the nozzle centerline. Dimensions of the deflectors (ref. 4) are given in figure 4. The bottom of the nozzle exhaust plane was located 0.1 chord (flaps retracted) above the wing/flap surface for each wing.

Wings

The model wings used in the studies are shown schematically in figure 5, together with pertinent dimensions. Details of their construction are given in reference 2. The wing chords with flaps retracted were 22.0, 33.0, and 49.5 cm. Herein, these wings are referred to as 2/3-baseline, baseline, and 3/2-baseline, respectively. The wing models represent the upper surface contours of an airfoil with 20° (takeoff) and 60° (approach) deflected flaps.

The following table summarizes the axial locations of the various nozzle types on the wings for the aeroacoustic test program.

Nozzle type	Wing	Flap angle, deg	Nozzle location, % chord re wing chord with retracted flaps
Slot and slot/deflector	2/3-Baseline	20	21,46
	Baseline	20	↓
	3/2-Baseline	20	
	2/3-Baseline	60	
	Baseline	60	
	3/2-Baseline	60	
Circular/deflector	2/3-Baseline	20	-----
	Baseline	20	10,21
	3/2-Baseline	20	10
	2/3-Baseline	60	-----
	Baseline	60	10,21
	3/2-Baseline	60	10

DATA NORMALIZATION

Lift and Thrust Characteristics

All of the slot and slot/deflector nozzle configurations had weight flow losses as reported in reference 1. In order to make meaningful comparisons of the lift and thrust data, all the configurations are compared on the basis of equal weight flow. This was achieved by adjusting the measured static lift and thrust by the ratio of the nozzle ideal weight flow to the nozzle actual weight flow for each configuration tested. The adjusted lift and thrust were then ratioed to the ideal nozzle-alone thrust giving the following expressions for the normalized lift and thrust:

$$\frac{L(W_i/W)}{T_i} \quad \text{and} \quad \frac{T(W_i/W)}{T_i}$$

All symbols are defined in the nomenclature.

Acoustic

The acoustic performance of the slot nozzles, when the aerodynamic performance is normalized on an equal weight flow basis, must also be adjusted for this normalization. In order to establish the necessary acoustic normalization, additional 40/40 slot nozzles of 16- and 30-percent greater area were tested with the baseline and 3/2-baseline wings. This nozzle was selected because it has the greatest weight flow loss. The 30-percent area increase was required in order to have a measured weight flow equal to that calculated for ideal flow of the initial 40/40 nozzle flow in the presence of the wing (ref. 1). On the basis of these tests it was found that the increase in noise caused by increasing the nozzle area in proportion to the weight flow could be determined by the following scaling relationship:

$$\Delta \text{ dB} = 10 \log (W_i/W)^{L_s/14}$$

The correction to the model scale spectral data given by the preceding equation was applied to all the slot nozzle/wing data, both with and without an external deflector. No correction was necessary for the data obtained with the conical/deflector nozzle configurations because no significant weight flow losses were incurred.

ANALYSIS

In order to obtain full-scale perceived noise levels, PNL, the model scale noise spectra were frequency shifted and amplitude corrected on a Strouhal basis. The typical portion of the model-scale spectra applicable to the full-scale spectral analysis is shown in figure 6 for a wing/flap configuration using a slot nozzle and one using a circular/deflector nozzle using a 13:1 scale factor for full-scale, and beginning the full-scale spectra at 50 Hz results in the utilization of the model-scale spectral data only for frequencies greater than 630 Hz. The spectra shown are for a measured radiation angle of 90° and at jet exhaust Mach number of 0.8. The data shown are for a takeoff mode (20° flap angle) with the baseline wing.

From full-scale spectra, such as those shown in figure 6, PNL values were computed at a flyover height of 152 m. These PNL values were computed at the model-scale test angles and then adjusted appropriately for the takeoff and approach attitudes shown in figure 7. Also shown in figure 7 are the flap angles associated with the operational mode of an aircraft.

Typical plots of PNL as a function of flyover distance for a wing/flap configuration using a circular/deflector nozzle are shown in figure 8. The two sets of data for both operational attitudes shown are for nominal jet exhaust velocities of 195 and 260 m/s. For the data shown, the PNL values near the overhead position ($\theta = 90^{\circ}$) are lower for the approach attitude than those for the takeoff attitude, by about 3 PNdB. However, in the forward arc ($\theta = 30^{\circ}$ to 50°) the PNL values are somewhat higher for the approach attitude than those for the takeoff attitude. This results in a larger duration term (see the appendix) in the calculation of the flyover relative noise level for the approach attitude than that for the takeoff attitude.

From plots of full-scale PNL values as a function of flyover distance (152 m altitude) a flyover relative noise level was computed as described in appendix A. The term "relative" is used herein since the conventional definition of effective perceived noise level (EPNL) includes forward flight effects, whereas the present data are for static conditions. The omission of flight effects, however, does not significantly affect the present flyover relative noise level comparisons between the various configurations. The flyover relative values were then plotted in terms of thrust and lift ratios, $T(W_i/W)/T_i$ and $L(W_i/W)/T_i$, respectively. From such plots, comparisons of relative flyover noise level for the various nozzle/wing configurations were made at essentially equal magnitudes of configuration lift and thrust.

PNL TRENDS

The PNL envelopes for all the nozzle/wing configurations are shown in figure 9 as a function of flyover distance for the three wing sizes included in the study. The data shown do not account for differences in lift and thrust ratios.

In general, increasing the wing size from 22 to 49.5 cm reduces the peak PNL 15 to 20 PNdB for the takeoff case (fig. 9(a)) due to increased jet noise shielding benefits associated with a larger wing. The largest reductions in PNL occur approximately ±125 m ($50^{\circ} \leq \theta \leq 130^{\circ}$) from the overhead position, with the maximum occurring directly overhead (90°). At greater ground flyover distances, the reduction in PNL with increased wing size over this same range is limited to less than 4 PNdB. It is also evident from the figure, that the reduction in peak PNL associated with increased wing size are accompanied by greater exposure durations (greater ground distances) relative to the highest respective PNL values. This is apparent from the flattening of the PNL curve with distance in the region of peak PNL values. Consequently, the relative noise level benefits afforded by a reduction in peak PNL due to jet noise shielding and reduced flap trailing edge velocities with increasing wing size are partly negated by a greater exposure distance (time).

For the approach case (fig. 9(b)) similar trends to those discussed for the takeoff case were obtained. However, in the approach case, the reduction in peak PNL values with increased wing size was only 1/3 to 2/3 those for the takeoff case. One factor influencing this reduction in peak PNL with increased wing size was the shift in peak PNL from directly overhead (90°) to a lower angle (50° to 70°) for the largest wing tested. This forward shift of the peak PNL value is attributed to flow interaction noise associated with the large nozzle roof angles or deflector angles needed to maintain flow attachment for the approach condition, particularly for certain nozzle/wing size combinations (see also ref. 1).

Finally, except for the largest wing size, the peak PNL values for the takeoff condition in general are about 4 to 5 PNdB greater than those for the approach condition. Except for the angular shift in the peak PNL location for the largest wing, the peak PNL values are substantially the same for both the takeoff and approach conditions.

Within each envelope, differences in PNL values caused by nozzle chordwise location and nozzle configuration were obtained. These differences are summarized in the following sections.

Nozzle Geometry/Acoustic Trends

Effect of roof/deflector angle. - In general, the effect of roof angle on the PNL values was negligible for the slot nozzles and the slot nozzles with sidewall cutback. For the nozzle/deflector configurations the PNL increased slightly, less than 2 PNdB, with decreasing deflector angles for the configurations tested. These trends were observed for both the takeoff and approach conditions.

Effect of nozzle chordwise location. - For the takeoff condition (20° flap angle) the PNL values were at substantially the same levels for the 10 and 21 percent chordwise locations of a particular nozzle configuration. With the nozzles located at 46 percent of chord, the PNL values were up to 5 PNdB greater than at the other two chordwise locations for the same nozzle configuration. Similar trends were evident for the approach condition (60° flap angle); however, the PNL difference between the nozzle location at 46 percent of chord and that at 10 or 21 percent of chord was generally less than 3 PNdB for the same nozzle configuration.

Effect of nozzle configuration. - The effect of nozzle configuration on the PNL values was most apparent with the nozzle located at 21 percent of the wing chord (fig. 10). It is evident that the slot nozzle with external deflector had the lowest PNL values in the range from $\theta = 50^{\circ}$ to 130° for the takeoff condition. However, the Δ PNL values between nozzle configurations increased with increasing wing chord. These trends occurred for both takeoff and approach attitudes. For the limited changes in nozzle configurations available for the 46 percent chord location of the nozzles no significant changes in PNL were observed for the available configurations. Also, the circular/deflector nozzle showed no significant PNL changes with nozzle location at 10 or 21 percent and chord sizes of 33.0 and 49.5 cm.

AEROACOUSTIC PERFORMANCE COMPARISONS

General

Acoustic data were obtained for most nozzle configurations with the baseline wing and for many of the nozzle configurations with the 2/3- and 3/2-scale wings. Similarly, aerodynamic data were obtained for most nozzle configurations with the baseline wing. On the basis of these data, only those nozzle configurations showing good aerodynamic performance were further evaluated with the 2/3- and 3/2-baseline wings.

In figures 11 and 12 the flyover relative noise levels (FRNL) for each of the nozzle/wing configurations are shown as a function of the thrust ratio, $T(W_i/W)/T_i$ and the lift ratio, $L(W_i/W)/T_i$. The variation for each nozzle/wing configuration

results from the effects of nozzle roof/deflector size and angles, and for various chordwise locations of the nozzles. For the takeoff attitude (20° flap angle), decreasing the nozzle roof/deflector angle results in both thrust and lift ratios increasing up to the point at which the jet flow separates from the flap surface. After flow separation occurs, the lift ratio decreases while the thrust ratio continues to increase with further decreases in roof/deflector angles. For the approach attitude (60° flap angle) decreasing the roof/deflector angle again results in an increase in thrust ratio; however, the lift ratio decreases for the slot-type nozzles. With those nozzles using deflectors, the lift ratio increases for the baseline wing but decreases for the 3/2-baseline wing as the nozzle roof/deflector angle is decreased. A change in jet exhaust velocity from 260 to 195 m/s does not change the general trends just discussed.

Takeoff Attitude

The flyover relative noise levels for the takeoff attitude are shown in figure 11 as a function of thrust and lift ratios.

For peak aeroacoustic performance comparisons with the baseline wing (fig. 11(b)), a nominal thrust ratio of 0.82 and the associated nominal lift ratio of 0.43 were selected. At these values, the appropriate circular/deflector nozzles are about 2.5 dB quieter than the slot-type. Locating the slot-type nozzles at 46-percent chord increases the noise level (FRNL) by a further 2.5 dB from that obtained at 21-percent chord. At the selected peak thrust and lift ratios, the slot/deflector nozzle, located at 21-percent chord, showed an aeroacoustic performance comparable to that for the circular/deflector nozzle. However, with the slot/deflector nozzle located at 46-percent chord, the thrust ratio was considerably less (up to 8 percent) than that obtained with the slot nozzles at the same chord location.

Aeroacoustic data for the slot-type nozzles only are available with the 2/3-baseline wing (fig. 11(a)). These data show that the same difference in noise level exist between chord locations of 21 and 46 percent as with the baseline wing. The data also show that the noise level with the 2/3-baseline wing is 3 dB louder than that with the baseline wing for the same nozzles and chord locations. Also, the peak lift ratio is about 2.5 percent lower with the short wing compared with that for the baseline wing; the thrust ratios with the two wings was about the same.

With the 3/2-baseline wing, the nominal thrust ratio at which acoustic comparisons could be made was 0.78 while the associated nominal lift ratio was 0.43. At these levels it is apparent that the nozzle configurations tested differ little in

noise level, with a maximum difference of only 2 dB for those shown. The noise levels shown are about 7 dB less for the slot-nozzles than those obtained with the baseline wing. For the circular/deflector nozzles, the noise levels are 3.5 to 5.5 dB less than those with the baseline wing.

A change in jet Mach number from 0.8 to 0.6 did not change the relative differences between the nozzle configurations.

Approach Attitude

The flyover relative noise levels for the approach attitude are shown in figure 12 as a function of thrust and lift ratios.

For aeroacoustic performance comparisons with the baseline wing (fig. 12(b)), a nominal thrust ratio of 0.48 and the associated nominal lift ratio of 0.69 were selected. At these values, the slot-type nozzle configuration, with the nozzle at 21-percent chord, has the lowest lift ratio (0.66) whereas the remaining nozzle configurations group between 0.69 and 0.72. Also, the slot-type nozzles shown had sidewall cutback in order to provide flow attachment to the wing/flap surfaces. At the selected peak thrust/lift ratios, the slot/deflector nozzle located at 21-percent chord did not attain the levels of the other nozzles configurations, being about 4 percent lower. Similarly, the lift ratio was lower than most of the other nozzle configurations. The noise levels for the slot/deflector nozzles were about the same as that for the slot-type nozzles at their respective peak thrust and lift ratios. With the slot/deflector nozzles located at 46-percent chord, the aeroacoustic performance was about the same as that for the slot-type nozzles at the same location and the circular/deflector nozzles at 10- and 21-percent chord. The maximum FRNL difference between the various nozzles, at the selected thrust and lift ratios, is 3.5 dB.

Comparing the preceding FRNL values with those for takeoff shows that the noise level of the circular/deflector nozzles is substantially independent of flap angle (operational attitude). However, the slot-type nozzles are significantly quieter for the approach attitude than for the takeoff attitude, by up to about 6 dB.

With the 2/3- and 3/2-baseline wings (figs. 12(a) and 12(c), respectively), data trends with nozzle configurations and nozzle chord location similar to those discussed for the takeoff attitude were obtained. However, with the 2/3-baseline wing, the approach attitude FRNL values were up to 3 dB quieter than those for the takeoff attitude at the respective representative lift and thrust ratios. With the 3/2-baseline wing, the FRNL values were up to 2 dB noisier than those for the takeoff attitude at the respective representative lift and thrust ratios.

As in the case for the takeoff attitude, a change in jet Mach number from 0.8 to 0.6 did not change the relative differences between the nozzle configurations.

CONCLUDING REMARKS

On the basis of the aeroacoustic data presented herein, it appears that an above-the-wing mounted circular nozzle with an external flow deflector merits further study when its performance is compared with slot-type nozzles for OTW-STOL applications, particularly in view of noise reduction benefits in the takeoff attitude. The present work also indicates that variable geometry (nozzle roof/deflector angle) is desirable for optimizing the aeroacoustic performance. Finally, as has been shown in the literature but not discussed herein, the use of vortex generators on the wing surface to promote jet exhaust flow attachment to the flap surface for the approach attitude (large flap angles) is recommended. Their use, by providing better flow attachment should yield greater lift ratios than reported herein and may further reduce the approach attitude noise levels.

NOMENCLATURE

A, B, C, X, Y, y	local component dimensions (see fig. 5)
c_a	speed of sound in air
D	diameter
D_t	duration term
d	flight path distance from aircraft overhead point
EPNL	effective perceived noise level
FRNL	flyover relative noise level
H	aircraft altitude
h	source distance from microphone line (analogous to altitude, A)
L	measured lift
L_f	projected surface distance from nozzle exit plane to wing leading edge (see fig. 5)
L_p	projected surface distance (see fig. 5)
L_s	surface distance measured from nozzle exit plane to flap trailing edge (see fig. 5)

ℓ_f	deflector lip chord
ℓ_p	propagation path length
ℓ_T	distance from nozzle exit to deflector trailing edge (see fig. 5)
M_j	jet exhaust Mach number
M_o	aircraft Mach number
PNL	perceived noise level
PNLT	tone corrected perceived noise level
SPL	measured sound pressure level
T	measured thrust
T_i	ideal thrust
t	time
V	aircraft speed
W	measured weight flow
W_i	ideal weight flow
X	distance along microphone line measured from $\theta = 90^o$ (analogous to flight path distance, d)
β	roof/deflector angle
γ	nozzle sidewall cutback angle
θ	aircraft attitude corrected emission angle

APPENDIX - FLYOVER RELATIVE NOISE LEVEL

by Francis J. Montegani

The practical noise reduction value of acoustic changes observed in static tests is properly established by scaling the data in frequency and level to full scale (engine size), postulating a flyover situation, and computing flyover noise. This requires lengthy calculations and a description of the flyover conditions. The flyover noise concept is used here to establish a simpler procedure that can be applied to static data, independently of flight considerations, to obtain a relative measure of the implied effect on flyover noise. The procedure generates what is here termed flyover relative noise level (FRNL). Differences in flyover relative noise levels computed from static test data, adjusted to full scale in frequency only are equivalent to differences that will result in effective perceived noise level (EPNL) for constant flyover conditions.

Effective perceived noise level as defined by FAR-36 (ref. 5) is expressed as the sum of the maximum tone-corrected perceived noise level and a duration correction. The expressions given in FAR-36 can easily be rewritten to obtain the same result expressed as the antilog-mean tone-corrected perceived noise level during the period when it is within 10 dB of the maximum value plus a differently defined duration term. Thus,

$$\mathrm{EPNL} = \overline{\mathrm{PNLT}} + D_t \tag{1}$$

where

$$\overline{\mathrm{PNLT}} = 10 \log\left\{ \frac{1}{t_2 - t_1} \int_{t_1}^{t_2} 10^{\left[\frac{\mathrm{PNLT}(t)}{10}\right]} dt \right\} \tag{2}$$

$$D_t = 10 \log\left(\frac{t_2 - t_1}{10}\right) \tag{3}$$

and t_1, t_2 are the time limits in seconds between which the tone-corrected perceived noise level is within 10 dB of the maximum value.

Consider the geometry of an aircraft level flyover as illustrated in figure A1. If $t = 0$ corresponds to the instant when the aircraft is directly above an observer, the time at which the observer receives noise emitted from the aircraft at an angle θ is

$$t = \frac{d}{V} + \frac{\ell_p}{C_a} \tag{4}$$

where d is the distance along the flight path from the overhead point to the aircraft (with due regard for sign), V is the aircraft speed, ℓ_p is the propagation path length, and C_a is the ambient speed of sound. The first term is the time required for the aircraft to travel from the overhead point to the place at which the acoustic ray emitted at the angle θ intercepts the observer. The second term is the time of acoustic propagation from the aircraft to the observer along the ray. In terms of the angle θ, this can be rewritten as

$$t = \frac{H}{V}\left(\frac{1}{\tan\theta} + \frac{M_o}{\sin\theta}\right) \tag{5}$$

where H is the aircraft altitude and M_o is the aircraft Mach number. For the usual aircraft speeds at approach and takeoff, and at angles associated with noise levels within 10 dB of maximum, the second term on the right of equation (5) can be neglected with small loss of accuracy.

Figure A2 illustrates the corresponding geometry associated with the static test noise data. The data from microphone measurements are known on a line at a distance h as a function of angle θ. (Data obtained from a circular measurement arc are easily adjusted to this form.) In terms of test variables, then, $\tan\theta$ in equation (5) is given by h/X. Equation (5), with the small term omitted, can thus be written

$$t = \frac{H}{V} \cdot \frac{X}{h} \tag{6}$$

Let X_1 and X_2 denote the distances on the line where the tone-corrected perceived noise levels are 10 dB below maximum. The corresponding time duration associated with these locations when the data are applied to a flyover situation is, from equation (6),

$$t_2 - t_1 = \frac{H}{Vh}(X_2 - X_1) \tag{7}$$

Substitution of the time duration into equation (3) yields, after expansion

$$D_t = 10 \log\left(\frac{H}{Vh}\right) + 10 \log(X_2 - X_1) - 10 \tag{8}$$

Equation (1) now can be written, after rearrangement

$$EPNL - 10 \log\left(\frac{H}{Vh}\right) - 10 = \overline{PNLT} + 10 \log(X_2 - X_1) \tag{9}$$

The left side of equation (9) is effective perceived noise level as defined by FAR-36 normalized by quantities that are constant for given flyover and static test geometries. It represents effective perceived noise level to within an additive constant so that for sets of test data it is a relative measure of flyover noise. The terminology flyover relative noise level, FRNL, is adopted, and equation (9) is written

$$FRNL = \overline{PNLT} + 10 \log(X_2 - X_1) \tag{10}$$

The quantity $\overline{PNLT}$ is obtained from equation (2) after replacing t, which is a dummy variable of integration, with X. The limits t_1 and t_2 defining the 10 dB-down points are correspondingly replaced with X_1 and X_2. The units of X_1 and X_2 are arbitrary since different choices introduce an additive constant into equation (10), which has no effect on differences in values of flyover relative noise level.

The expression for relative flyover noise level can thus be written for static test noise data as

$$FRNL = 10 \log\left\{\frac{1}{X_2 - X_1}\int_{X_1}^{X_2} 10^{\left[\frac{PNLT(X)}{10}\right]} dx\right\} + 10 \log(X_2 - X_1) \tag{11}$$

This can be simplified finally to

$$FRNL = 10 \log\left\{\int_{X_1}^{X_2} 10^{\left[\frac{PNLT(X)}{10}\right]} dx\right\} \tag{12}$$

Note that equation (12) is a measure of the area under the antilog tone-corrected perceived noise level data curve as a function of X between the 10 dB-down limits.

REFERENCES

1. U. von Glahn and D. Groesbeck, "Nozzle and Wing Geometry Effects on OTW Aerodynamic Characteristics," NASA TM X-73420 (1976).

2. U. von Glahn and D. Groesbeck, "Geometry Effects on STOL Engine-Over-the-Wing Acoustics with 5:1 Slot Nozzles," NASA TM X-71820 (1975).

3. U. von Glahn and D. Groesbeck, "OTW Noise Correlation for Several Nozzle/Wing Geometries Using a 5:1 Slot Nozzle with External Deflectors," NASA TM X-73529 (1976).

4. U. von Glahn and D. Groesbeck, "Effect of External Jet-Flow Deflector Geometry on OTW Aero-Acoustic Characteristics," NASA TM X-73460 (1976).

5. "Noise Standards: Aircraft Type and Airworthiness Certification," Federal Aviation Regulations, Part 36, Federal Aviation Administration, Washington, D.C. (1974 as amended).

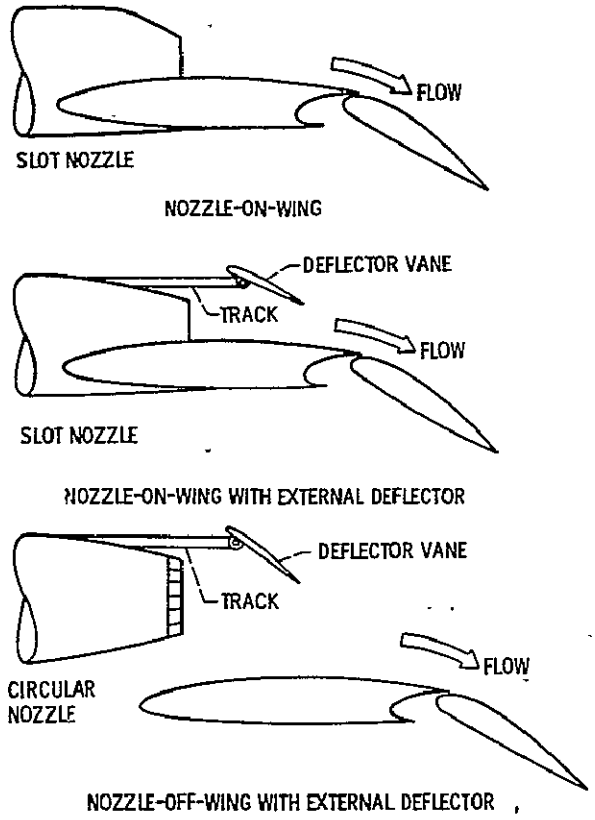

Figure 1. - Conceptual OTW nozzle/wing configurations.

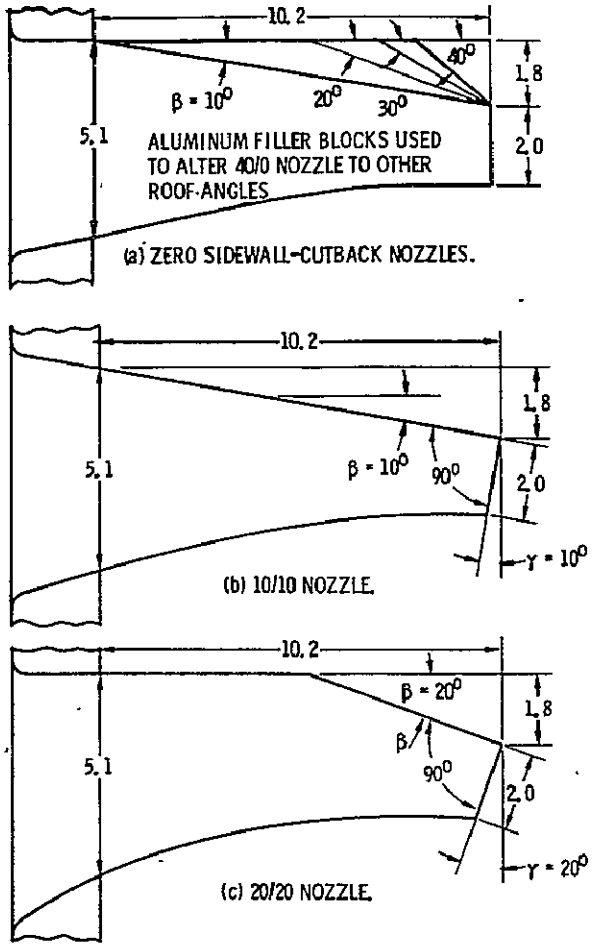

Figure 2. – Sketches of slot nozzles, with and without sidewall cutback. Dimensions in centimeters. All nozzles 10.2 centimeters wide.

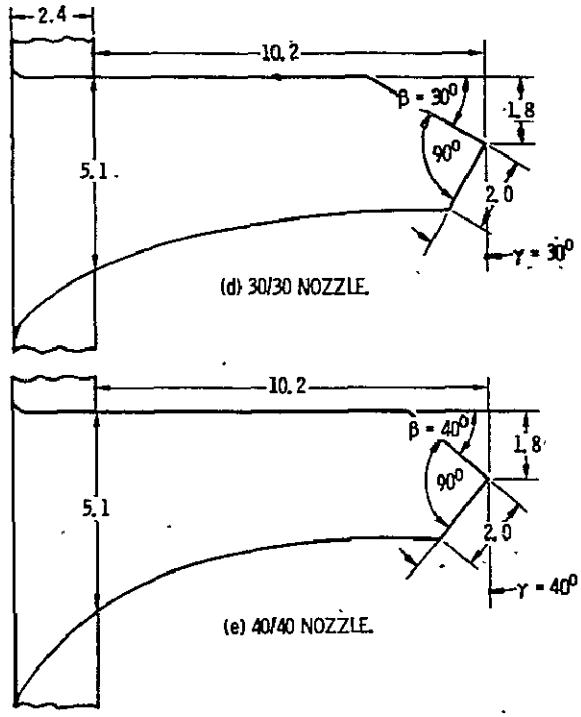

Figure 2. - Concluded.

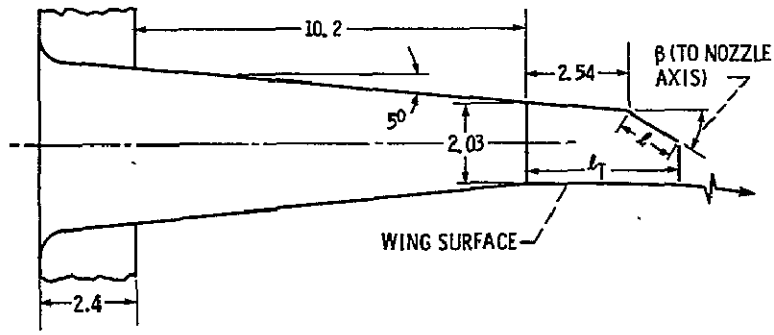

DEFLECTOR ANGLE, β, deg	DEFLECTOR LIP, ℓ, cm	TOTAL DEFLECTOR LENGTH, ℓ_T, cm	REFERENCE
40	1.27	3.61	3
30	1.59	4.06	3
30	1.27	4.01	-
25	↓	4.0	-
20	↓	4.04	-
15	↓	4.09	-
40	0.64	3.25	3
30	↓	3.25	-
25	↓	3.30	-
20	↓	3.35	-
15	↓	3.30	-

Figure 3. - Sketch of 5:1 slot/deflector nozzle. Dimensions in centimeters. All deflectors were 15.2 cm wide. Nozzle width is 10.2 cm.

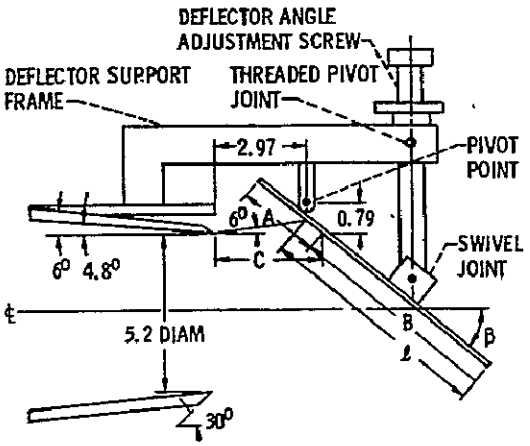

ℓ	A	B	C	β
4.14	2.51	3.18	3.91	20°
	2.29	3.40	3.66	25°
	2.18	3.51	3.51	30°
	2.06	3.63	3.25	40°
7.90	2.54	6.91	4.01	20°
	2.31	7.14	3.66	25°
	2.11	7.34	3.40	30°
	2.03	7.42	3.18	40°

Figure 4. – Schematic sketch of circular nozzle and flow deflectors. Dimensions in centimeters.

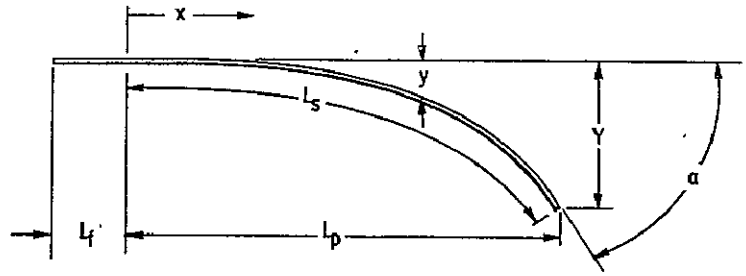

WING COORDINATES

FLAP ANGLE, α, DEG	WING CONFIGURATION	x/L_p / y/Y	0-0.4	0.5	0.6	0.7	0.8	0.9	0.95	0.975	1.0
20	2/3-BASELINE, BASELINE		0	0.04	0.13	0.26	0.44	0.70	0.85	-----	1.0
	3/2-BASELINE		0	0.025	0.10	0.225	0.42	0.70	0.85	-----	1.0
60	ALL		0	0.02	0.055	0.125	0.24	0.44	0.61	0.76	1.0

WING DIMENSIONS

FLAP ANGLE, α, DEG	WING SIZE	NOZZLE LOCATION, % CHORD	Y, cm	L_f, cm	L_p, cm	L_s, cm
20	2/3-BASELINE	21	4.4	4.6	22.5	23.3
		46		10.2	16.9	17.8
	BASELINE	10	6.6	3.3	37.4	39.0
		21		6.9	33.8	35.4
		46		15.2	25.4	27.0
	3/2-BASELINE	10	10.2	5.0	56.0	58.4
		21		10.2	50.8	53.2
		46		22.9	38.1	40.6
60	2/3-BASELINE	21	9.6	4.6	20.3	25.7
		46		10.2	14.7	20.3
	BASELINE	10	14.3	3.3	34.1	42.3
		21		6.9	30.5	38.7
		46		15.2	22.1	30.2
	3/2-BASELINE	10	21.5	5.0	50.9	62.8
		21		10.2	45.7	57.6
		46		22.9	33.1	45.1

Figure 5. - Model-scale wing dimensions and coordinates. Dimensions in centimeters.

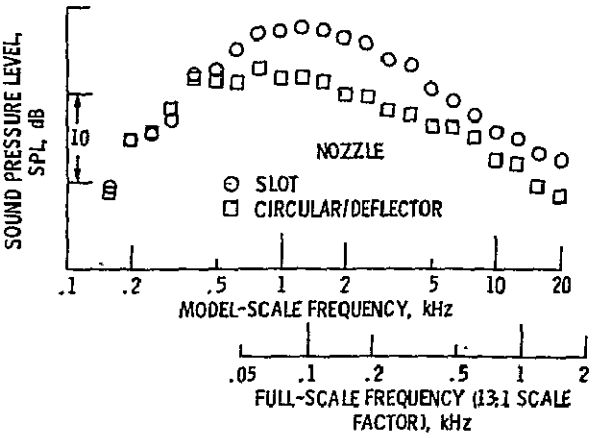

Figure 6. - Illustration of typical model-scale acoustic spectra applicable to present full-scale OTW noise studies. Measured radiation angle, 90°; jet Mach no., 0.8; baseline wing, 20° flap deflection.

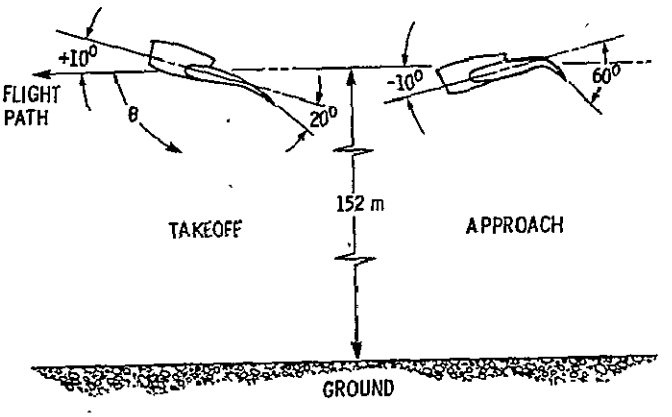

Figure 7. - Schematic of nozzle/wing orientation used for configuration aeroacoustic comparisons.

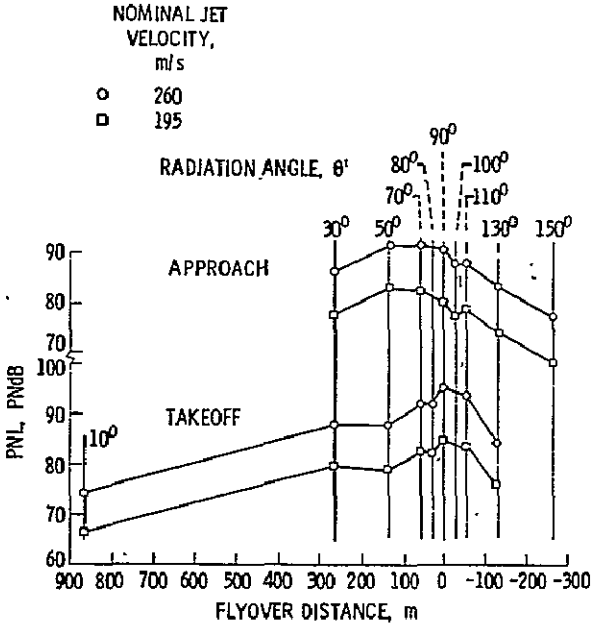

Figure 8. - Typical PNL variations with flyover distance. Circular/deflector nozzle; deflector length, 53.8 cm; deflector angle, 30°; baseline wing, nozzle at 10% chord; 152 m altitude.

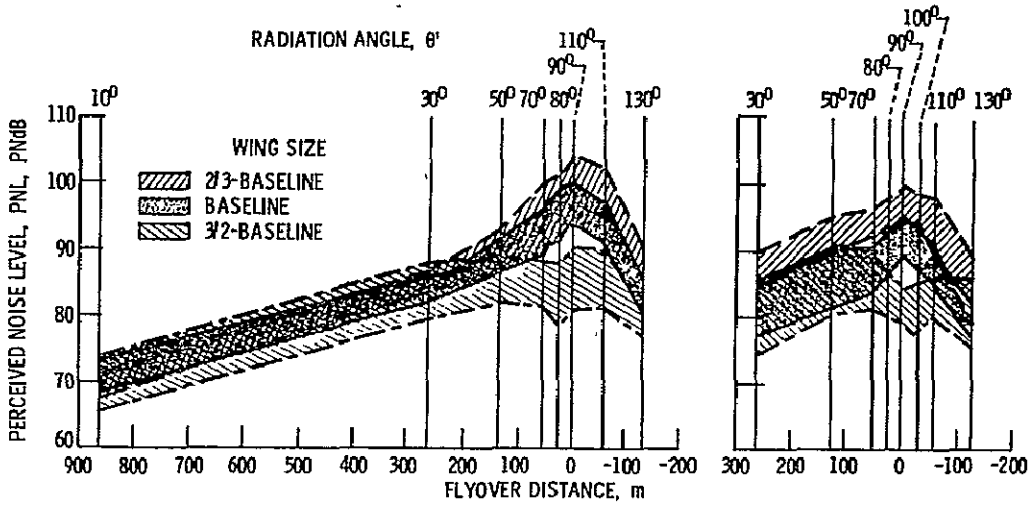

(a) TAKEOFF ATTITUDE (20° FLAP ANGLE).

(b) APPROACH ATTITUDE (60° FLAP ANGLE).

Figure 9. - PNL envelopes for various nozzle/wing configurations. Jet Mach no., 0.8.

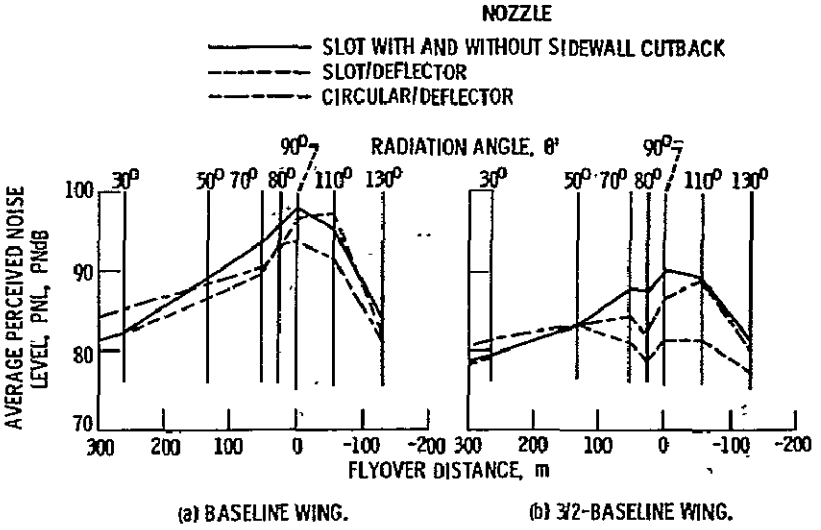

(a) BASELINE WING. (b) 3/2-BASELINE WING.

Figure 10. - Effect of nozzle configuration on PNL. Takeoff attitude (20° flap deflection); jet Mach no., 0.8, nozzle at 21% chord.

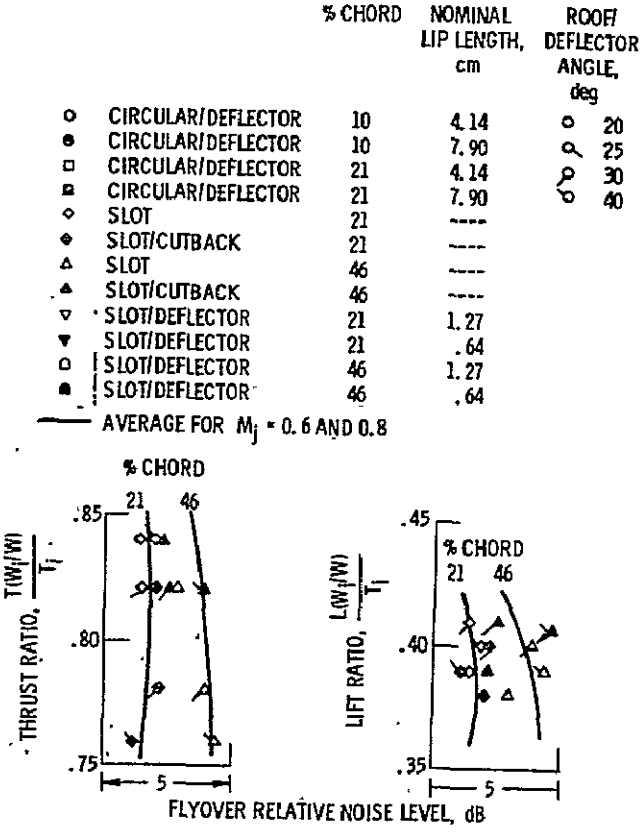

(a) 2/3-BASELINE WING.

Figure 11. - Variation of flyover relative noise level with lift and thrust ratios for takeoff attitude (20° flap angle). Jet Mach no., 0.8.

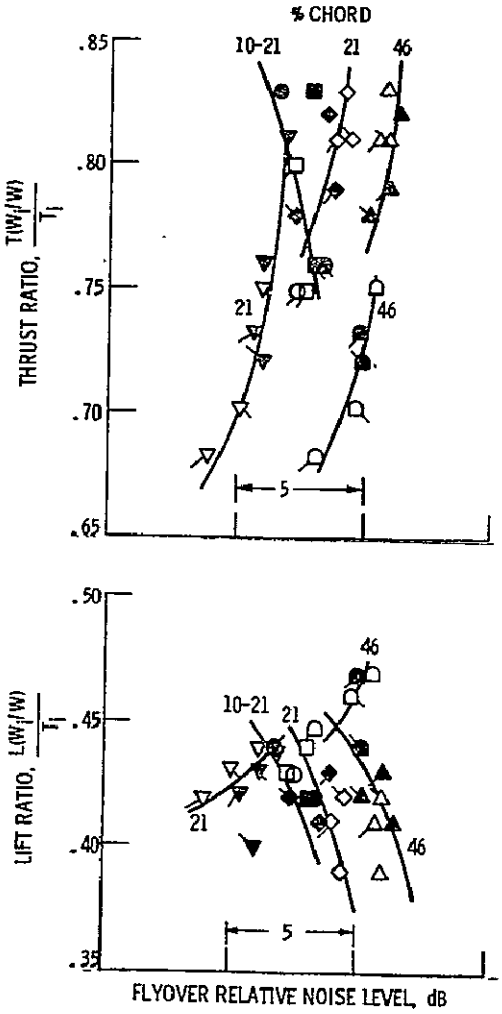

(d) BASELINE WING.

Figure 11. - Continued.

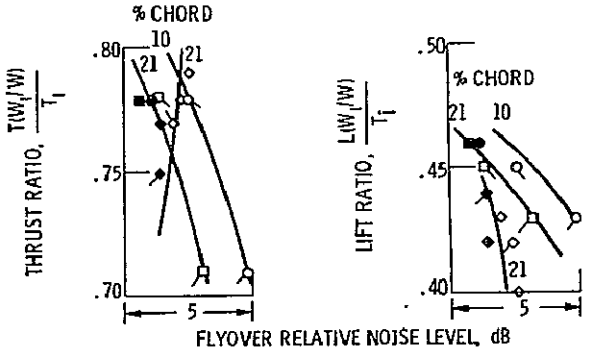

(c) 3/2-BASELINE WING.

Figure 11. - Concluded.

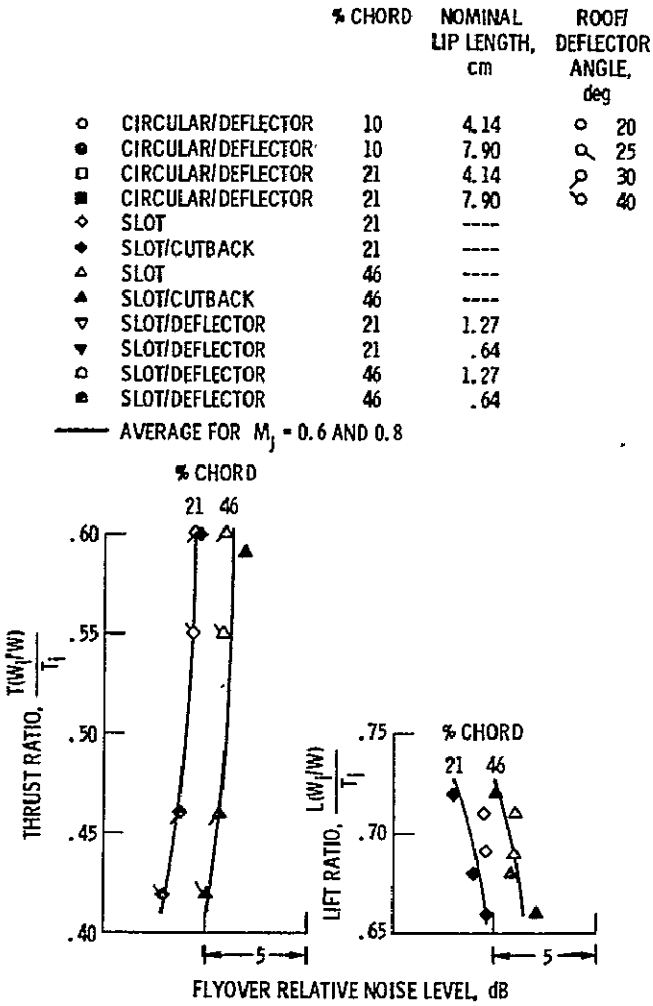

(a) 2/3-BASELINE WING.

Figure 12. – Variation of flyover relative noise level with lift and thrust ratios for approach attitude (60^{0} flap angle). Jet Mach no., 0.8.

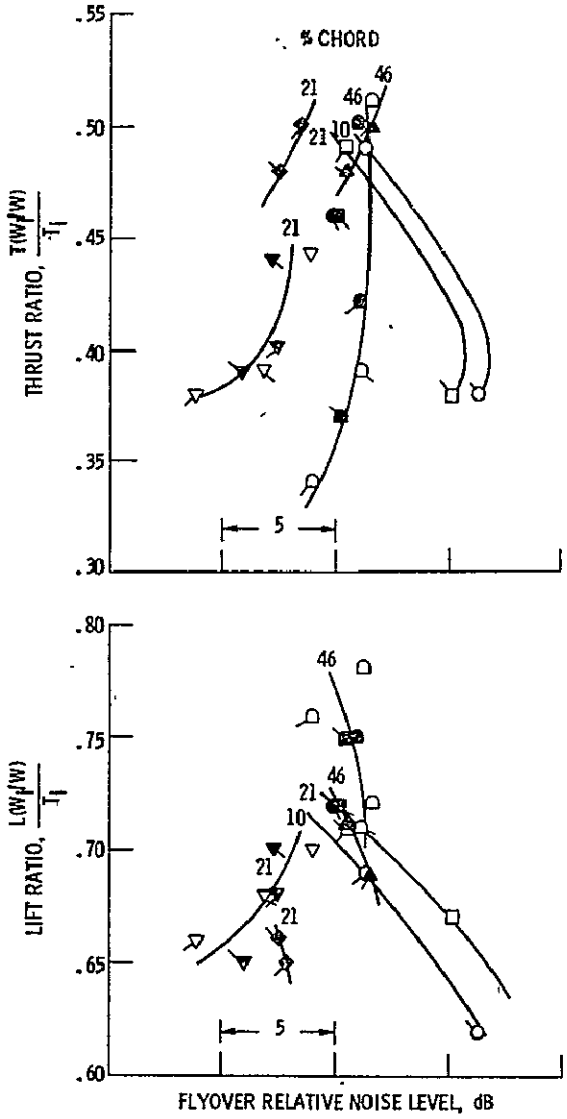

(b) BASELINE WING.

Figure 12. - Continued.

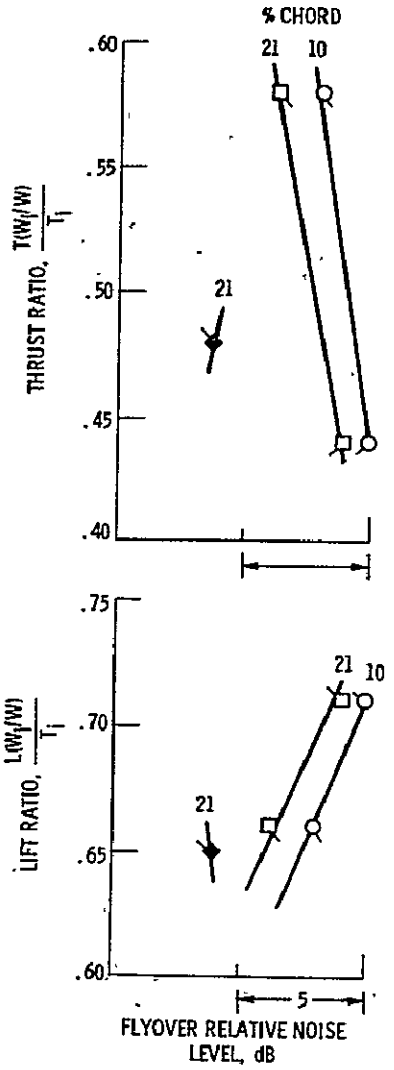

(c) 3/2-BASELINE WING.

Figure 12. - Concluded.

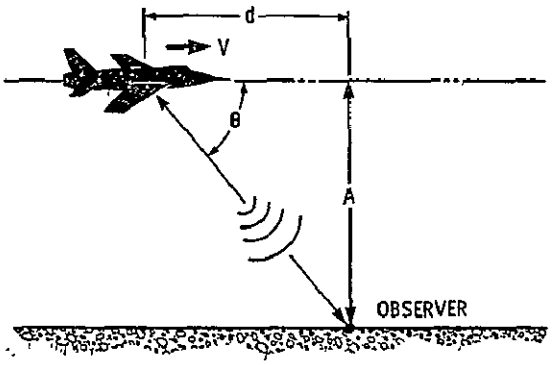

Figure A1. - Flyover geometry

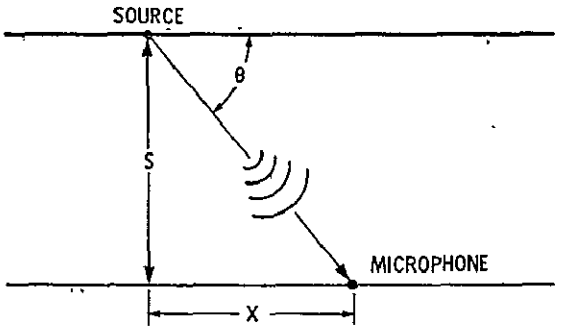

Figure A2. - Static test geometry.

1. Report No NASA TM-79168	2 Government Accession No	3 Recipient's Catalog No
4 Title and Subtitle ASSESSMENT AT FULL SCALE OF NOZZLE/WING GEOMETRY EFFECTS ON OTW AEROACOUSTIC CHARACTERISTICS		5 Report Date 6 Performing Organization Code
7. Author(s) D. Groesbeck and U. von Glahn		8. Performing Organization Report No E-031 10 Work Unit No
9 Performing Organization Name and Address National Aeronautics and Space Administration Lewis Research Center Cleveland, Ohio 44135		11 Contract or Grant No 13 Type of Report and Period Covered Technical Memorandum
12 Sponsoring Agency Name and Address National Aeronautics and Space Administration Washington, D.C. 20546		14. Sponsoring Agency Code

15 Supplementary Notes

Appendix - Flyover Relative Noise Level by Francis J. Montegani.

16 Abstract

The effects on acoustic characteristics of nozzle type and location on a wing for STOL engine over-the-wing configurations are assessed at full scale on the basis of model-scale data. Three types of nozzle configurations are evaluated: a circular nozzle with external deflector mounted above the wing, a slot nozzle with external deflector mounted on the wing and a slot nozzle mounted on the wing. Nozzle exhaust plane locations with respect to the wing leading edge are varied from 10 to 46 percent chord (flaps retracted) with flap angles of 20^{o} (takeoff attitude) and 60^{o} (approach attitude). Perceived noise levels (PNL) are calculated as a function of flyover distance at 152 m altitude. From these plots, static EPNL values, defined as flyover relative noise levels, are calculated and plotted as a function of lift and thrust ratios. From such plots the acoustic benefits attributable to variations in nozzle/deflector/wing geometry at full scale are assessed for equal aerodynamic performance.

17 Key Words (Suggested by Author(s)) Jet noise shielding Jet noise	18 Distribution Statement Unclassified - unlimited STAR Category 71		
19 Security Classif (of this report) Unclassified	20 Security Classif (of this page) Unclassified	21. No. of Pages	22 Price*

* For sale by the National Technical Information Service, Springfield, Virginia 22161

National Aeronautics and Space Administration

Washington, D.C.
20546

Official Business
Penalty for Private Use, $300

SPECIAL FOURTH CLASS MAIL
BOOK

Postage and Fees Paid
National Aeronautics and
Space Administration
NASA-451

POSTMASTER: If Undeliverable (Section 158 Postal Manual) Do Not Return